

MEVITA: Open-Source Bipedal Robot Assembled from E-Commerce Components via Sheet Metal Welding

Kento Kawaharazuka^{*1}, Shogo Sawaguchi^{*1}, Ayumu Iwata¹,
Keita Yoneda¹, Temma Suzuki¹, and Kei Okada¹

Abstract—Various bipedal robots have been developed to date, and in recent years, there has been a growing trend toward releasing these robots as open-source platforms. This shift is fostering an environment in which anyone can freely develop bipedal robots and share their knowledge, rather than relying solely on commercial products. However, most existing open-source bipedal robots are designed to be fabricated using 3D printers, which limits their scalability in size and often results in fragile structures. On the other hand, some metal-based bipedal robots have been developed, but they typically involve a large number of components, making assembly difficult, and in some cases, the parts themselves are not readily available through e-commerce platforms. To address these issues, we developed MEVITA, an open-source bipedal robot that can be built entirely from components available via e-commerce. Aiming for the minimal viable configuration for a bipedal robot, we utilized sheet metal welding to integrate complex geometries into single parts, thereby significantly reducing the number of components and enabling easy assembly for anyone. Through reinforcement learning in simulation and Sim-to-Real transfer, we demonstrated robust walking behaviors across various environments, confirming the effectiveness of our approach. All hardware, software, and training environments can be obtained from github.com/haraduka/mevita.

I. INTRODUCTION

A wide range of bipedal robots has been developed over the years [1]–[11]. Traditionally, these robots have relied on harmonic drives as their primary gear mechanism [1]–[7]. However, with recent advancements in motor technology, actuators with low gear reduction ratios have become mainstream [8]–[11]. Such low-gear-ratio robots have made it easier to bridge the gap between simulation and the real world, enabling the application of reinforcement learning to achieve stable walking behaviors [10], [12], [13].

In parallel, a variety of learning methods – including imitation learning, reinforcement learning, and foundation model-based approaches – have recently been released as open-source software, creating an environment in which anyone can easily apply these learning techniques. This open-source wave is also extending into robotic hardware. In recent years, several open-source hardware platforms have been developed for quadrupedal robots [14]–[17] and bipedal robots [18]–[23]. While some of these robots provide access to their design files [24], [25], they do not fully adhere to the formal definition of open-source [26].

^{*} K. Kawaharazuka and S. Sawaguchi contributed equally to this work.

¹ The authors are with the Department of Mechano-Informatics, Graduate School of Information Science and Technology, The University of Tokyo, 7-3-1 Hongo, Bunkyo-ku, Tokyo, 113-8656, Japan. [kawaharazuka, sawaguchi, a-iwata, k-yoneda, t-suzuki, k-okada]@jsk.imi.i.u-tokyo.ac.jp



Fig. 1. MEVITA – Open-source bipedal robot easily constructed through e-commerce with sheet metal welding and machining, developed in this study.

In this study, we focus specifically on open-source bipedal robots. Most existing open-source bipedal robots [18]–[20], [23] are designed with 3D printing in mind. While 3D printing offers advantages in terms of ease of fabrication, cost, and geometric flexibility, it poses limitations in terms of structural strength, making it difficult to scale up or enable dynamic, high-intensity motions. In contrast, a few metal-based open-source bipedal robots have also been developed [21], [22]. However, due to the reliance on traditional metal machining, these robots often consist of many components, making them difficult to assemble. Additionally, the required parts are not always available through e-commerce platforms.

To address these issues, we developed MEVITA, an open-source bipedal robot whose entire frame is composed of metal and whose mechanical and electronic components can be fully sourced from e-commerce platforms. In particular, by utilizing MISUMI and its online manufacturing service

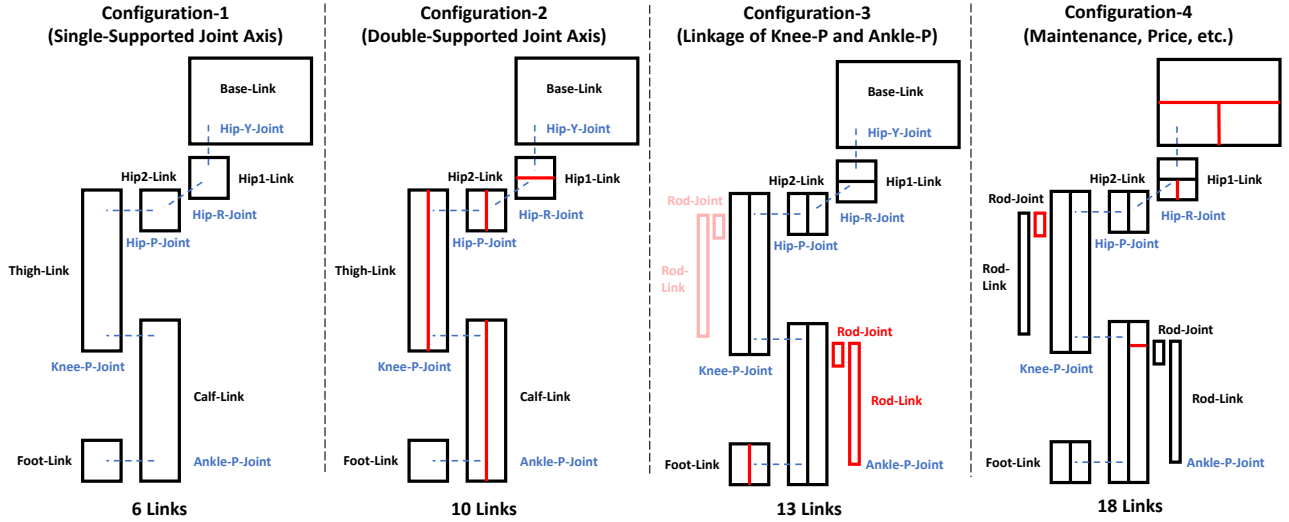


Fig. 2. The number of link components in a bipedal robot's various minimal configurations: Configuration-1 represents the case where all joints are single-supported; Configuration-2 assumes all joints except the Hip-Y joint are double-supported; Configuration-3 introduces parallel linkages at the Knee-P and Ankle-P joints; and Configuration-4 corresponds to the design adopted in MEVITA, taking into account factors such as maintenance and cost.

mevity [27], we enabled the procurement of not only bearings and shafts but also all structural links and joint components directly from e-commerce platforms. Furthermore, we propose a design principle based on minimizing the number of components, from the minimal viable configuration to a fully functional bipedal robot. Although designing freeform geometries is more challenging with metal compared to 3D printing, we addressed this by employing sheet metal welding to integrate complex geometries into single components. As a result, MEVITA achieves a significant reduction in the number of parts compared to previous robots, allowing for an easily assemblable design. Excluding mirrored components, MEVITA's skeletal frame consists of only 18 unique metal parts. Despite its simple CAN-based circuit architecture, MEVITA is capable of robust walking across diverse environments, enabled by reinforcement learning in simulation and Sim-to-Real transfer.

II. DESIGN AND CONFIGURATION OF MEVITA

A. Minimum Design of Bipedal Robots

First, we consider the minimal configuration of a bipedal robot. In this study, we focus on a 5-DoF leg configuration that excludes the ankle roll joint, following the design of robots such as Duke Humanoid [22], Cassie [28], and MIT Humanoid [29]. Each leg, therefore, consists of a 3-DoF hip joint, a 1-DoF knee joint, and a 1-DoF ankle joint. The order of the three DoFs in the hip joint can vary depending on the robot, with examples such as Y-R-P [1], [2], [22], [29], R-Y-P [28], and P-R-Y [10], where R, P, and Y denote roll, pitch, and yaw joints, respectively. In this work, we adopt the most widely used Y-R-P order. Note that the number of components required for the minimal configuration is unaffected by the chosen joint order.

The left side of Fig. 2 shows Configuration-1, which represents the minimal structure of a bipedal robot. A robot with 5-DoF per leg and a Y-R-P hip structure has the

following joints: Hip-Y, Hip-R, Hip-P, Knee-P, and Ankle-P. To connect these joints, six links are needed: Base, Hip1, Hip2, Thigh, Calf, and Foot. Thus, considering just one leg and the torso, six links form the minimal configuration.

Configuration-2 builds upon Configuration-1 by converting the single-supported (cantilevered) joints into more practical double-supported structures. Since the Hip-Y joint generally experiences less torque, it is common to apply double support only to the Hip-R, Hip-P, Knee-P, and Ankle-P joints. As a result, the Hip1, Hip2, Thigh, and Calf links become two-part assemblies, bringing the total to ten distinct link components in the minimal double-supported configuration.

In recent bipedal robot designs, to increase leg agility, Configuration-3 introduces parallel link mechanisms at the Knee-P and Ankle-P joints. This allows the motors to be positioned more proximally, thereby reducing the link's moment of inertia. To implement this, two additional components are required: a Rod-Joint attached to the motor and a parallel Rod-Link forming the linkage (ideally shared for both Knee-P and Ankle-P). Furthermore, to implement a double-supported Rod-Link, the Foot-Link must be split into two parts (whereas the split in the Calf-Link from earlier can be reused for the Knee-P joint). Although the Rod-Joint should also be split for double support, since it is a small component mounted at the motor's tip, it can be designed as a single piece while maintaining double support. Therefore, Configuration-3, which includes both double-supported structures and parallel links, results in a minimal configuration consisting of 13 distinct link components.

Finally, considering factors like maintenance and material cost, MEVITA adopts Configuration-4, consisting of 18 components. While 13 components represent the theoretical minimum in Configuration-3, realizing this in practice is difficult. This is because each individual part becomes very large, resulting in higher costs and reduced maintainability. Therefore, in Configuration-4, the Base-Link is split into

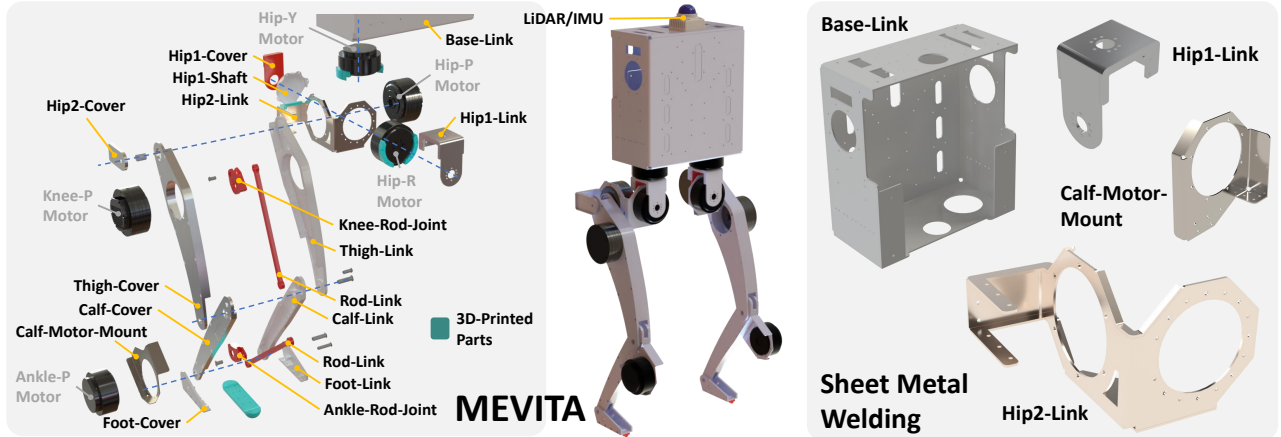


Fig. 3. Design overview of MEVITA: excluding mirrored parts, the robot consists of 18 unique metal components, four of which are fabricated using sheet metal welding to achieve complex and large geometries as single integrated parts.



Fig. 4. All metal components used in MEVITA.

three parts – a main body, a cover, and a battery access hatch – to improve maintainability and ease of battery removal. Similarly, the Hip1-Link and Calf-Link are each split into three parts to reduce material costs by keeping individual components smaller. To account for the different torque requirements at the Knee-P and Ankle-P joints, we use separate motors for each and thus design the Rod-Joint as two distinct components. Consequently, MEVITA’s Configuration-4 comprises 18 unique link components. On the other hand, even with just these 18 parts, it is quite challenging to fabricate all of them solely through simple machining. Large structural components would require extensive material removal if machined from solid blocks, leading to excessive cost and production time. In practice, such components are usually subdivided further to facilitate efficient manufacturing. In this study, we instead explored the use of sheet metal welding to construct complex shapes as single integrated parts.

B. Design Overview of MEVITA

An overview of the MEVITA design is shown in Fig. 3, and all the metal components used are shown in Fig. 4. MEVITA features five degrees of freedom per leg. The Hip-P and Knee-P joints use T-MOTOR AK10-9 actuators, while the Hip-Y, Hip-R, and Ankle-P joints use T-MOTOR AK70-10. All structural components of MEVITA are made from either aluminum or stainless steel. Machined metal parts use A7075, standard sheet metal parts are made of A5052, and

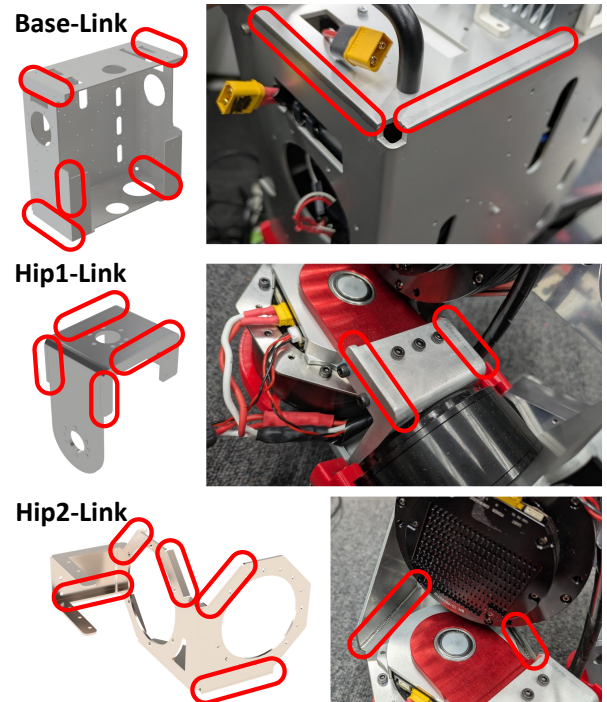


Fig. 5. Details of sheet metal welding for the Base-Link, Hip1-Link, and Hip2-Link. The welded sections are highlighted in red.

certain high-strength sheet metal components are fabricated from SUS304. Additional parts such as the foot sole and joint limiters are 3D-printed using TPU. Each link is divided into a *-Link and *-Cover to achieve a double-supported structure. Additionally, for cost reduction in Configuration-4, some new components – such as the Hip1-Shaft and Calf-Motor-Mount – have been introduced. As for sensors, a Livox Mid-360 is mounted on the top of the Base-Link. This sensor not only enables environmental perception and SLAM but also functions as an IMU for control purposes.

A key feature of MEVITA is that four of its link components – Base-Link, Hip1-Link, Hip2-Link, and Calf-Motor-

TABLE I
COMPARISON BETWEEN EXISTING BIPEDAL ROBOTS AND MEVITA

Name	Weight	Leg Length ^{*1}	Leg DoFs	Materials ^{*2}	Open/Closed (CAD)	Number of Metal Parts ^{*3}
Cassie [28]	33.32 kg	0.5 m	5	Metal	Closed	-
MIT Humanoid [9]	21 kg ^{*4}	0.28 m	5	Metal	Closed	-
Berkeley Humanoid [11]	16 kg	0.2 m	6	Metal	Closed	-
Bolt [20]	1.34 kg	0.2 m	3	Plastic	Open	-
Berkeley Humanoid Lite [23]	16 kg ^{*4}	0.16 m	6	Plastic	Open	-
Duke Humanoid [22]	30 kg	0.25 m	5	Metal	Open	24
MEVITA (This Study)	19.8 kg	0.32 m	5	Metal	Open	18

^{*1} The average of the link lengths of the thigh and calf links.

^{*2} The materials of the functional components forming the robot's skeletal structure.

^{*3} The number of the metal components forming the skeletal structure, excluding the mirror parts.

^{*4} Including the weight of the arms.

Mount – are constructed via sheet metal welding. The Base-Link and Hip1-Link are made from A5052, while the Hip2-Link and Calf-Motor-Mount are made from SUS304. As shown in Fig. 5, welding multiple sheet metal plates together allows the construction of highly complex shapes as single parts. In particular, the Base-Link is a single component that forms the entire torso, measuring 300×320×150 [mm]. The Hip2-Link is also a single part, formed by welding together four sheets to achieve a complex yet strong structure. These components are designed to be compatible with mevify, the manufacturing service provided by MISUMI [27], and can be automatically quoted and ordered through e-commerce using only STEP files.

C. Comparison with Existing Bipedal Robots

A comparison between MEVITA and existing bipedal robots is shown in Table I. The table compares seven robots, including MEVITA. Among them, Cassie [28], MIT Humanoid [9], and Berkeley Humanoid [11] are not open-source, while Bolt [20], Berkeley Humanoid Lite [23], Duke Humanoid [22], and MEVITA are open-source. Although the robots differ in weight, leg length, and number of leg DoFs, MEVITA has a leg length and weight relatively close to those of MIT Humanoid and Duke Humanoid. Among the open-source robots, Bolt and Berkeley Humanoid Lite are designed with 3D printing in mind. MEVITA, like the Duke Humanoid, is based on metal machining, but the number of metal parts in MEVITA has been reduced from 24 (in the Duke Humanoid) to 18. Considering the 13-part minimum configuration (Configuration-3) shown in Fig. 2, the Duke Humanoid adds 11 extra parts, while MEVITA adds only 5. This demonstrates that by incorporating sheet metal welding, MEVITA successfully limits the increase in part count to less than half compared to conventional metal-machined designs.

D. Circuit Configuration of MEVITA

The circuit configuration of MEVITA is shown in Fig. 6. MEVITA uses the NVIDIA Jetson Orin Nano Developer Kit as its onboard computer. Connected to it are two CAN-USB interfaces and a Livox Mid-360, a LiDAR sensor equipped with an IMU. Motor power is managed via a wireless emergency stop switch and a power relay. MEVITA is powered by LiPo batteries: two 24 V batteries are connected in series to

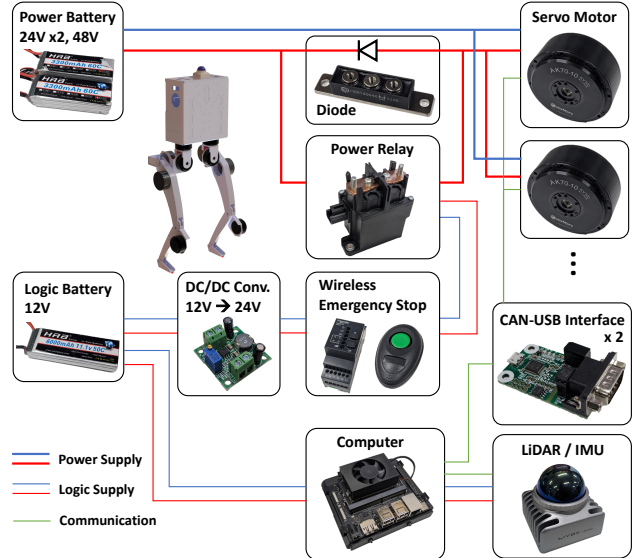


Fig. 6. Circuit configuration of MEVITA: servo motors are connected to the PC via two CAN-USB interfaces, and the system is equipped with a wireless emergency stop, power relay, diode, and LiDAR/IMU.

provide 48 V for the motors, while a separate 12 V battery is used for logic power supply. The actual internal layout of MEVITA's electronics inside the Base-Link is shown in Fig. 7. The LiPo battery is centrally located, with other devices arranged around it with sufficient clearance, making future expansion relatively easy.

E. Control Architecture of MEVITA

The control architecture of MEVITA is illustrated in Fig. 8. MEVITA's control is primarily based on reinforcement learning using IsaacGym / LeggedGym [30]. The learned policy is first validated through Sim-to-Sim transfer using MuJoCo [31], and then finally tested on the real hardware. The control input consists of joint angle commands for PID control. The state vector includes the angular velocity and gravity direction vector of the Base-Link, the desired velocity command for the Base-Link, joint positions, and joint velocities. The reward function is adapted from those commonly used for quadrupedal locomotion tasks and applied to the bipedal context. To enable Sim-to-Real

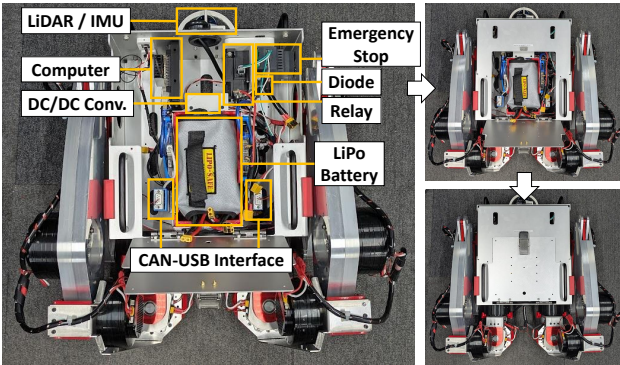


Fig. 7. The actual circuit layout inside MEVITA’s Base-Link.

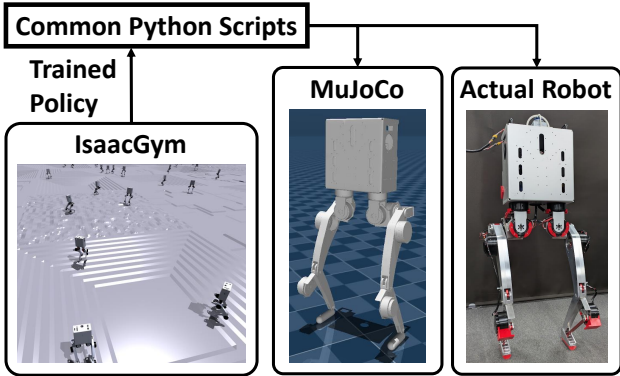


Fig. 8. Control system of MEVITA: policies trained in IsaacGym are verified in MuJoCo and deployed to the actual hardware using common Python scripts.

transfer, a variety of domain randomization techniques are employed. These include noise added to the mass, moment of inertia, and center of mass of each link, as well as to friction coefficients and control command latency. For further details, please refer to the learning environment software available at github.com/haraduka/mevita.

III. EXPERIMENTS

First, we evaluated the differences observed when deploying a policy trained in IsaacGym to both MuJoCo simulation and the physical MEVITA robot. Fig. 9 shows the tracking performance when the robot was commanded to follow linear and angular velocity inputs in forward, lateral, and rotational directions. The results indicate that the robot generally follows the commanded velocities and angular velocities in both simulation and the real world. In particular, the tracking of rotational commands shows minimal discrepancy between simulation and hardware. On the other hand, for translational velocity commands, the real robot exhibits slightly larger errors compared to the simulation.

Next, Fig. 10 shows walking experiments conducted in various environments. These include (A) uneven indoor terrain, (B) grass field, (C) dirt surface, (D) concrete tiles, and (E) a gentle slope. In all of these environments, MEVITA demonstrated stable walking behavior.

On the other hand, it is difficult to say that the motion is

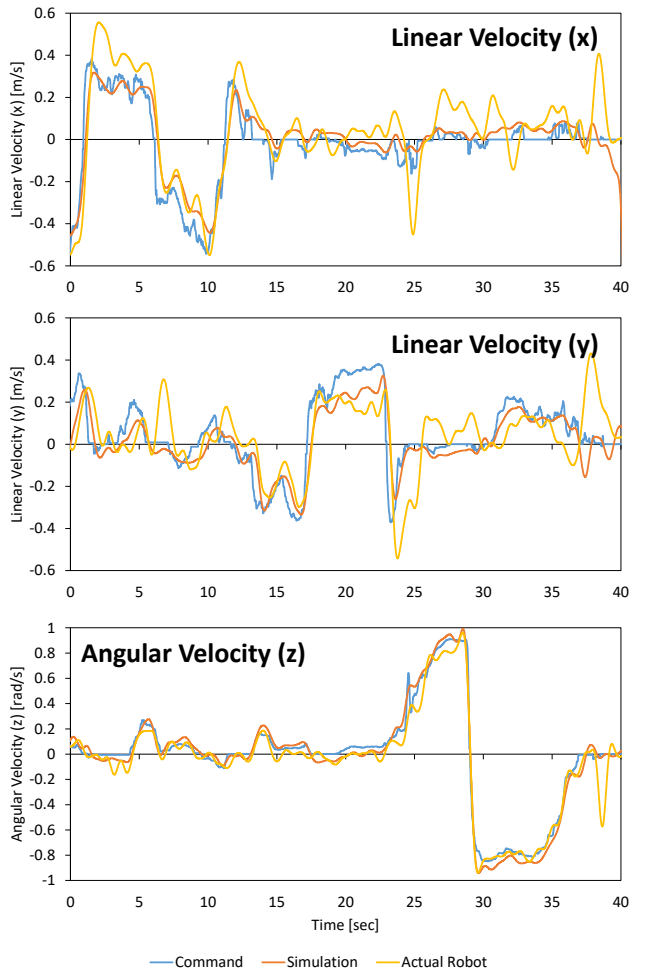


Fig. 9. Comparison of the tracking performance to the target commands when applying the trained policy to both MuJoCo simulation and the actual robot.

completely stable. In particular, the robot is currently more unstable when standing still than when walking, indicating a need for policy adjustments. Additionally, excessive speed can lead to falls, and during lateral movements, the feet may get caught on the ground. Going forward, it will be necessary to carefully consider both Sim-to-Real and Real-to-Sim transfer to achieve more stable walking.

IV. CONCLUSION

In this study, we developed MEVITA, an open-source bipedal robot composed of metal components, all of which can be sourced from e-commerce platforms. One of the main challenges in metal-based open-source bipedal robots is the increased number of components due to the difficulty of fabricating freeform geometries. We addressed this by considering the minimal structural configuration and employing sheet metal welding to integrate multiple parts into single components. As a result, MEVITA achieves a significant reduction in the number of components compared to existing open-source bipedal robots, enabling an easily assemblable design that anyone can build with readily available parts. Despite its simple circuit architecture, MEVITA is capable of



Fig. 10. Walking experiments in various environments: (A) uneven indoor terrain, (B) grassy field, (C) dirt surface, (D) concrete tiles, and (E) a gentle slope.

performing stable walking behaviors in various environments through reinforcement learning in simulation and Sim-to-Real transfer. By fully making all components open-source, we hope MEVITA will lower the barrier to bipedal robot development and contribute to the further advancement of research in physical intelligence.

REFERENCES

- [1] K. Hirai, M. Hirose, Y. Haikawa, and T. Takenaka, "The Development of Honda Humanoid Robot," in *1998 IEEE International Conference on Robotics and Automation*, 1998, pp. 1321–1326.
- [2] K. Kaneko, F. Kanehiro, S. Kajita, H. Hirukawa, T. Kawasaki, M. Hirata, K. Akachi, and T. Isozumi, "Humanoid robot HRP-2," in *2004 IEEE International Conference on Robotics and Automation*, 2004, pp. 1083–1090.
- [3] A. Parmiggiani, M. Maggiali, L. Natale, F. Nori, A. Schmitz, N. Tsagarakis, J. S. Victor, F. Becchi, G. Sandini, and G. Metta, "The design of the iCub humanoid robot," *International Journal of Humanoid Robotics*, vol. 9, no. 04, p. 1250027, 2012.
- [4] N. G. Tsagarakis, S. Morfey, G. M. Cerda, L. Zhibin, and D. G. Caldwell, "COMpliant huMANoid COMAN: Optimal joint stiffness tuning for modal frequency control," in *2013 IEEE International Conference on Robotics and Automation*, 2013, pp. 673–678.
- [5] J. Englsberger, A. Werner, C. Ott, B. Henze, M. A. Roa, G. Garofalo, R. Burger, A. Beyer, O. Eiberger, K. Schmid, and A. Albu-Schaffer, "Overview of the torque-controlled humanoid robot TORO," in *2014 IEEE-RAS International Conference on Humanoid Robots*, 2014, pp. 916–923.
- [6] N. G. Tsagarakis, D. G. Caldwell, F. Negrello, W. Choi, L. Baccelliere, V.-G. Loc, J. Noorden, L. Muratore, A. Margan, A. Cardellino, *et al.*, "WALK-MAN: A High-Performance Humanoid Platform for Realistic Environments," *Journal of Field Robotics*, vol. 34, no. 7, pp. 1225–1259, 2017.
- [7] P. Seiwald, S.-C. Wu, F. Sygulla, T. F. Berninger, N.-S. Staufenberg,

- M. F. Sattler, N. Neuburger, D. Rixen, and F. Tombari, "LOLA v1.1—An Upgrade in Hardware and Software Design for Dynamic Multi-Contact Locomotion," in *2020 IEEE-RAS International Conference on Humanoid Robots*, 2021, pp. 9–16.
- [8] Y. Liu, J. Shen, J. Zhang, X. Zhang, T. Zhu, and D. Hong, "Design and Control of a Miniature Bipedal Robot with Proprioceptive Actuation for Dynamic Behaviors," in *2022 IEEE International Conference on Robotics and Automation*, 2022, pp. 8547–8553.
- [9] A. SaLoutos, E. Stanger-Jones, Y. Ding, M. Chignoli, and S. Kim, "Design and development of the mit humanoid: A dynamic and robust research platform," in *2023 IEEE-RAS International Conference on Humanoid Robots*, 2023, pp. 1–8.
- [10] "G1 (Unitree Robotics)," <https://m.unitree.com/g1>.
- [11] Q. Liao, B. Zhang, X. Huang, X. Huang, Z. Li, and K. Sreenath, "Berkeley humanoid: A research platform for learning-based control," *arXiv preprint arXiv:2407.21781*, 2024.
- [12] I. Radosavovic, T. Xiao, B. Zhang, T. Darrell, J. Malik, and K. Sreenath, "Real-world humanoid locomotion with reinforcement learning," *Science Robotics*, vol. 9, no. 89, p. eadi9579, 2024.
- [13] A. Tang, T. Hiraoka, N. Hiraoka, F. Shi, K. Kawaharazuka, K. Kojima, K. Okada, and M. Inaba, "HumanMimic: Learning Natural Locomotion and Transitions for Humanoid Robot via Wasserstein Adversarial Imitation," in *2024 IEEE International Conference on Robotics and Automation*, 2024, pp. 13 107–13 114.
- [14] J. Kim, T. Kang, D. Song, and S. Yi, "PAWDQ: A 3D Printed, Open Source, Low Cost Dynamic Quadruped," in *2021 International Conference on Ubiquitous Robots*, 2021, pp. 217–222.
- [15] F. Grimminger, A. Meduri, M. Khadiv, J. Viereck, M. Wthrich, M. Naveau, V. Berenz, S. Heim, F. Widmaier, T. Flayols, J. Fiene, A. Badri-Sprwitz, and L. Righetti, "An Open Torque-Controlled Modular Robot Architecture for Legged Locomotion Research," *IEEE Robotics and Automation Letters*, vol. 5, no. 2, pp. 3650–3657, 2020.
- [16] P. Léziart, T. Flayols, F. Grimminger, N. Mansard, and P. Souères, "Implementation of a Reactive Walking Controller for the New Open-Hardware Quadruped Solo-12," in *2021 IEEE International Conference on Robotics and Automation*, 2021, pp. 5007–5013.
- [17] K. Kawaharazuka, S. Inoue, T. Suzuki, S. Yuzai, S. Sawaguchi, K. Okada, and M. Inaba, "MEVIUS: A Quadruped Robot Easily Constructed through E-Commerce with Sheet Metal Welding and Machining," in *2024 IEEE-RAS International Conference on Humanoid Robots*, 2024, pp. 631–636.
- [18] M. Lapeyre, P. Rouanet, J. Grizou, S. Nguyen, F. Depraetere, A. Le Falher, and P.-Y. Oudeyer, "Poppy project: open-source fabrication of 3D printed humanoid robot for science, education and art," in *2014 International Conference on Digital Cultures*, 2014, pp. 1–6.
- [19] P. Allgeuer, H. Farazi, M. Schreiber, and S. Behnke, "Child-sized 3D printed igus humanoid open platform," in *2015 IEEE-RAS International Conference on Humanoid Robots*, 2015, pp. 33–40.
- [20] E. Daneshmand, M. Khadiv, F. Grimminger, and L. Righetti, "Variable Horizon MPC with Swing Foot Dynamics for Bipedal Walking Control," *IEEE Robotics and Automation Letters*, vol. 6, no. 2, pp. 2349–2356, 2021.
- [21] Y. Huang, Y. Zeng, and X. Xiong, "STRIDE: An Open-Source, Low-Cost, and Versatile Bipedal Robot Platform for Research and Education," in *2024 IEEE-RAS International Conference on Humanoid Robots*, 2024, pp. 402–409.
- [22] B. Xia, B. Li, J. Lee, M. Scutari, and B. Chen, "The Duke Humanoid: Design and Control For Energy Efficient Bipedal Locomotion Using Passive Dynamics," *arXiv preprint arXiv:2409.19795*, 2024.
- [23] Y. Chi, Q. Liao, J. Long, X. Huang, S. Shao, B. Nikolic, Z. Li, and K. Sreenath, "Demonstrating Berkeley Humanoid Lite: An Open-source, Accessible, and Customizable 3D-printed Humanoid Robot," *arXiv preprint arXiv:2504.17249*, 2025.
- [24] G. Ficht, P. Allgeuer, H. Farazi, and S. Behnke, "NimbRo-OP2: Grown-up 3D Printed Open Humanoid Platform for Research," in *2017 IEEE-RAS International Conference on Humanoid Robots*, 2017, pp. 669–675.
- [25] H. Shi, W. Wang, S. Song, and C. K. Liu, "ToddlerBot: Open-Source ML-Compatible Humanoid Platform for Loco-Manipulation," *arXiv preprint arXiv:2502.00893*, 2025.
- [26] "The Open Source Definition," <https://opensource.org/osd>.
- [27] "meviy (MISUMI)," <https://meviy.misumi-ec.com/worldwide/en/>.
- [28] J. Reher, W.-L. Ma, and A. D. Ames, "Dynamic Walking with Compliance on a Cassie Bipedal Robot," in *18th European Control Conference*, 2019, pp. 2589–2595.
- [29] M. Chignoli, D. Kim, E. Stanger-Jones, and S. Kim, "The MIT humanoid robot: Design, motion planning, and control for acrobatic behaviors," in *2020 IEEE-RAS International Conference on Humanoid Robots*, 2021, pp. 1–8.
- [30] N. Rudin, D. Hoeller, P. Reist, and M. Hutter, "Learning to walk in minutes using massively parallel deep reinforcement learning," in *2022 Conference on Robot Learning*, 2022, pp. 91–100.
- [31] E. Todorov, T. Erez, and Y. Tassa, "MuJoCo: A physics engine for model-based control," in *2012 IEEE/RSJ International Conference on Intelligent Robots and Systems*, 2012, pp. 5026–5033.